28 Mar 2001, 4:00 pm - 6:30 pm

The 1999 Athens (Greece) Earthquake: Energy and Duration-Related Response Spectral Characteristics of Different Site Conditions

P. K. Koliopoulos
Technological Education Institute of Serres, Greece

B. N. Margaris
Institute of Engineering Seismology and Earthquake Engineering (ITSAK), Greece

The 1999 Athens (Greece) Earthquake: Energy and Duration - Related Response Spectral Characteristics of Different Site Conditions.

P.K. Koliopoulos
Technological Education Institute of Serres,
Department of Construction Engineering,
GR-62124 Serres, GREECE.

B.N. Margaris
Institute of Engineering Seismology and Earthquake Engineering (ITSAK),
46 Georgikis Scholis Str., P.O. Box 53,
GR-55102 Thessaloniki, GREECE

ABSTRACT

An earthquake of September 7, 1999 (M5.9) has occurred in the Athens (Attika) area and was felt in almost all central Greece. The earthquake caused a lot of damage and extensive loss of life. The most damaged region is located within a distance of 10 km from the epicenter and numerous modern buildings and industrial facilities collapsed. The accelerograms, which have been recorded during the main event, are processed and compared with the empirical predictive relations proposed for Greece. For each record, the bracketed and significant duration as well as various energy-related measures are estimated. The correlation of these measures with the macroseismic intensity of the particular accelerographic site is then examined. Thus, the destructiveness of the individual records, based solely on the analysis of the ground motion process, is established. The influence of duration and frequency content on structural damage is then incorporated into the response spectral values via the adoption of novel site-dependent probabilistic 3D-spectra. Finally all the above characteristics are compared in order to select the strong-motion properties and response spectral parameters that encapsulate the damage potential of the seismic action and therefore are best suited for design purposes.

INTRODUCTION

On September 7, 1999 at 14:56 local time (11:56 GMT) the city of Athens was hit by a strong earthquake, local magnitude, M_L 5.4 (M5.9). The geographical coordinates of the earthquake were 38.09° N and 23.63° E and its focal depth, h=14 km approximately. The epicenter of the main shock was located at the SW flank of the mountain Parnitha in the NW sector of the Greek capital, Athens, in which almost 4 millions habitants live there. The fault plane solution proposed by Harvard University (φ=114°, δ=45°, λ=-73°) indicated WNW-ESE trending, almost south-dipping normal fault.

The most heavily damaged area lies in the northern suburbs of Athens close to the causative fault. A number of modern buildings collapsed (more than 40 buildings) including a number of industrial installations, killing 143 people and injuring some hundreds of them. Additionally, hundrends of buildings experienced extended structural damage with a cost estimate of 4 billion US dollars. The most affected areas by the main-shock reported Modified Mercalli intensities varying from VI to IX. The strong motion of the main-shock was recorded by nine accelerographs belonging to the permanent strong motion network of Institute of Engineering Seismology and Earthquake Engineering (ITSAK) installed at various distances from the epicenter ranging from 15 km to 58 km. Three more accelerographs belonging to the Greek Public Power Corporation (PPC) installed at distances from 11 km to 57 km from the epicenter, registered the main-shock. The National Observatory in Athens (NOA) had installed, a special array in the new constructed subway in Athens, comprising 11 accelerographs in various levels from the surface and in distances from the epicenter between 14 km to 37 km [Anastasiadis *et al*, 1999]. Unfortunately, no recordings in near-field are available for direct assessment of the strong motion characteristics in the epicentral area. In Fig. 1 the broader seismic region is shown and the strong motion networks of the three aforementioned Organizations is included. Red triangles correspond to NOA network, green triangles depict the PPC network and the remaining triangles correspond to ITSAK network.

The reported soil conditions at the accelerographic sites show that the majority of the stations lay on soft rock or on shallow (less than 5m thick) deposits of firm soil overlying the rock [Psycharis *et al.*, 1999]. However a number of stations lay on deeper soil deposits, which may have amplified recorded motions at a range of frequencies between 3 to 15 Hz. A very limited geotechnical information is available for the strong motion accelerographic sites, and taking into account the surficial geologic description, the recording stations were classified herein in 3 different soil conditions: loose soil and shallow deposits (SC=0), firm soil overlying the rock (SC=1) and rock (SC=2).

All the above mentioned accelerographs have recorded the main-shock and a total number of 21 strong motion data were available for the study of the main event.

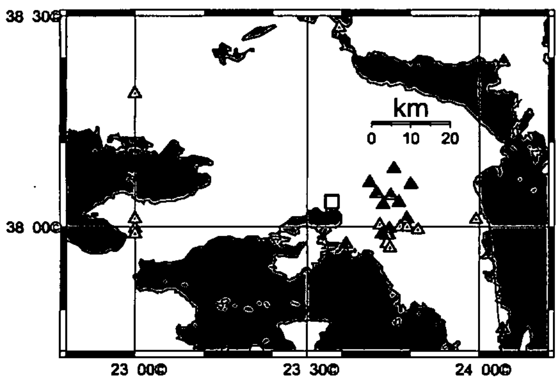

Fig. 1. The epicentral region and the surrounding areas of Athens earthquake 1999 including the strong-motion installations of ITSAK, NOA and PPC Organizations in Greece.

Although these records correspond to one seismic event, they exhibit considerable variability in terms of peak ground motion parameters (e.g., PGA, and PGV), duration measures (e.g., Husid duration, bracketed duration) and response spectral values(Table 1). Given the fact that the seismotectonic environment of the recording sites is identical, the above mentioned variability is mainly attributed to the influence of the local soil conditions.

In recent years, it has been recognized that the duration and the frequency content of the ground motion and of the corresponding response process are important parameters for the evaluation of the potential damage of the earthquake motion. Both parameters determine the number of visits (cycles) of the nonlinear response regime and influence the hysteretic damage accumulation. Unfortunately, these characteristics are not expressed in the conventional 2D response spectra and therefore, are not taken into account in the design process. Various alternative techniques have been suggested in the literature for the inclusion of these two characteristics in the seismic hazard and the structural analysis. These suggestions can be classified in two main categories. The first line of approach is focused on the development of energy related measures of the seismic action and the expression of the damagability of the ground motion in terms of functionals of these parameters [Uang and Bertero, 1990; Fajfar *et al*, 1990]. These parameters include, among others, the Housner Intensity index (related to the area under the pseudo-velocity response spectrum), the Fajfar Index (related to the PGV and the Husid duration) and the Total Energy Index (related to the energy induced by the earthquake action into the oscillating system). An extensive set of duration and energy characteristics regarding an ensemble of 201 Greek strong motion components has already been published [Koliopoulos *et al*, 1998] including comparisons with the Modified Mercalli Intensity, Imm, and providing regression functions that relate these parameters. It should be noted that there is no convincing method for the incorporation of these indices into the design process and their use is currently limited to the selection of a particular record with high damage potential, to be used in time history structural analysis.

A second line of approach, attempts the introduction of novel response spectra. Such attempts include, for example, the construction and use of the 2D Elastic inputenergy spectra for seismic hazard analysis [Chapman, 1999]. Although these energy spectra do incorporate the duration and the frequency content of the response process, are hard to interpret in terms of structural design code provisions. Another attempt, leads to a generalization of the conventional 2D response spectra into corresponding 3D-response spectra [Safak, 1998]. The third dimension is realized through the construction of a family of response spectra – in addition to the conventional single spectrum – by selecting the amplitudes of the second, third, fourth and so on, absolute response peaks. The plot of all the computed spectra, produce 3D response spectra in decreasing shape. The speed of the decay of the resulting surface is indicative of the persistence of the spectral response values. The volume under the 3D pseudo-velocity response spectrum has been reported to correlate well with computed damage indices of ten-story model building subjected to recorded ground motions from the Northridge earthquake [Safak, 1998]. This approach has the advantage that generalizes the familiar to the designers concept of response spectra and can be directly implemented in the design process producing duration and frequency consistent response spectra.

The present study treats 42 horizontal components of the 21 available strong ground motion records of the 1999 Athens earthquake. The particular records are listed in Table 1. The aim of the study is twofold. Firstly, certain duration and energy-related indices are computed and compared with earlier developed regression functions of these parameters based on past seismic events in Greece [Koliopoulos *et al*, 1998; Koutrakis, 2000]. Such a comparison is of particular importance as all the Athens records refer to the same event. Secondly, the novel 3D-response spectra methodology is implemented and its ability to incorporate information regarding duration, frequency content and damage potential is tested.

DURATION MEASURES

Firstly, the duration characteristics of the ground acceleration records were computed in terms of Husid Duration (HuDu in Table 1) which is the time needed for the accumulation of the 90% of the accelerogram intensity function I(t), defined as:

$$I(t) = \int_0^t a_g^2(t)\,dt \qquad (1)$$

Setting $t_{0.05}$ the time interval for the accumulation of the 5% of the total intensity and $t_{0.95}$ the corresponding time interval for the accumulation of the 95% of the total intensity, the Husid Duration is defined as:

$$HuDu = t_{0.95} - t_{0.05} \qquad (2)$$

A simple inspection of the computed Husid Duration of the various records (see Table 1) reveals the fact that records at distant sites with epicentral distance R>30Km (e.g. hal996, hal999, cor_ath, thi_ath, rfn) exhibit larger Husid Duration

TABLE 1. Accelerographic station codes, epicentral distances, depth of the instrument installation, soil conditions, macroseismic instensity, peak ground values, Husid duration, bracketed durations (L=0, 0.03 and 0.05 g), Housner instensity, total energy index, Fajfar intensity, deterministic 3D-spectral instensity (for 20 and 50 components), and probabilistic 3d-spectal intensity (11 conponents).

st_code	***r***	***l_a***	***SC***	***Imm***	***pga***	***pgv***	***HuDu***	***BrD0***	***BrD3***	***BrD5***	***I-H***	***TEI***	***I-F***	***3dvl50***	***3dvl20***	***3dprvl***
A299-1l	19.6	0	1	6	108.1	5.14	6.94	28.5	5.53	2.83	17.81	10.86	8.34	761	317	118
A299-1t	19.6	0	1	6	155.6	6.85	7.12	28.5	11.46	2.93	27.08	15.09	11.2	1178	486	190
a399-1l	15.3	0	1	7	258.6	16.08	5.85	39.1	12	11.52	55.67	25.16	25	2338	993	290
a399-1t	15.3	0	1	7	297.2	14.52	4.37	39.1	11.73	5.32	52.28	24.14	21	2147	919	280
a499-1l	16.2	0	1	6.5	118.6	8.9	6.5	27.4	3.52	2.59	28.62	14.44	14.2	1181	509	177
a499-1t	16.2	0	1	6.5	107.9	8.49	5.01	27.4	4.07	2.88	33.08	17.68	12.7	1459	604	234
cor_athl	57.5	0	0	4	33.47	1.77	18.46	26.6	0.04		6.65	5.15	3.7	284	119	47
cor_atht	57.5	0	0	4	23.6	1.35	20.61	26.6			5.72	4.86	2.9	248	103	42
thi_athl	36.3	0	2	4	40.26	1.82	15.04	32.2	1.08		9	6.5	3.6	394	164	62
thi_atht	36.3	0	2	4	32.7	1.7	18.01	32.2	2.35		8.63	7.27	3.5	388	158	66
hal996-1l	46	0	1	3	14.06	0.66	14.71	38.4			3.23	2.27	1.3	139	58	21
hal996-1t	46	0	1	3	15.53	0.5	16.78	38.4			2.69	2.21	1	118	49	19
hal999-1l	46	0	1	3	11.44	0.57	16.18	38.4			2.73	2.06	1.1	121	50	19
hal999-1t	46	0	1	3	10.36	0.52	16.97	38.4			2.52	2.12	1.1	114	46	19
aliv99-1l	57	0	2	3	19.95	0.91	10.73	29			3.44	2.16	1.6	147	62	22
aliv99-1t	57	0	2	3	16.35	0.9	10.6	29			3.2	1.94	1.6	134	57	21
kert99-1l	11.7	0	2	6.5	214.4	10.03	8.62	49.1	13.2	6.41	35.12	17.94	17.2	1420	615	174
kert99-1t	11.7	0	2	6.5	179.5	7.36	8.83	49.1	14.23	6.89	29.2	15.74	12.7	1192	510	148
lavr99-1l	55.2	0	2	4	41.58	1.98	10.94	35	2.85		7.79	3.82	3.6	315	135	44
lavr99-1t	55.2	0	2	4	51.97	1.8	11.15	35	1.77	0.01	6.25	3.09	3.3	250	109	32
atha1l	18.6	0	2	6	83.56	5.22	8.83	46	4.53	2.71	24.68	14.08	9	1113	456	161
atha1t	18.6	0	2	6	99.16	7.3	6.43	46	5.48	2.82	29.9	15.72	11.6	1326	645	184
dmk1l	23.1	0	2	5.5	49.91	2.37	13.58	40	2.66	0.01	10.23	6.52	4.5	457	186	74
dmk1t	23.1	0	2	5.5	69.87	2.4	11.59	40	2.43	1.88	10.1	5.84	4.4	421	176	62
mnsa1l	16.5	0	0	7	227.5	14.56	5.82	26.8	5.98	3.17	52.5	24.65	22.6	2184	950	305
mnsa1t	16.5	0	0	7	502	14.24	3.95	26.8	12.24	5.63	48.76	24.47	20.1	2000	845	308
rfn1l	37	0	1	4.5	81.39	2.85	8.35	22.2	1.56	1.08	11.27	8.81	4.8	478	201	77
rfn1t	37	0	1	4.5	101.4	4.17	6.11	22.2	2.57	1.16	15.38	8.06	6.6	655	278	101
splb1l	13.6	0	1	7	342	21.51	5.53	46	15.02	6.76	61.5	29.55	33	2625	1134	329
splb1t	13.6	0	1	7	318.9	18.73	5.6	46	14.12	5.49	63.13	29.55	28.8	2564	1094	317
dfna1l	19.1	-14	1	6	45.58	4.7	9.51	21	1.28		19.74	10.77	8.3	888	364	152
dfna1t	19.1	-14	1	6	77.93	6.9	6.49	21	1.97	0.4	27.75	15.21	11	1266	514	223
fix1l	17.8	-15	1	6.5	83.69	7.81	5.43	30	2.76	0.9	30.35	16.73	11.9	1390	564	228
fix1t	17.8	-15	1	6.5	121.6	11.04	5.26	30	3.68	1.03	29.12	14	16.7	1217	520	177
pnt1l	20.3	-15	1	6	85.32	7.51	8.56	30	3.29	2.89	32.67	17.45	12.8	1487	604	237
pnt1t	20.3	-15	1	6	77.49	5.13	8.32	30	2.18	0.68	21.15	11.62	8.7	919	384	138
sgma1l	16.9	-7	1	6.5	144.7	12.56	7.1	30	11.23	3.81	35.76	18.28	20.5	1556	648	239
sgma1t	16.9	-7	1	6.5	233.6	13.64	3.69	30	11.24	3.83	45.01	18.74	18.9	1770	800	240
sgmb1l	16.9	-26	1	6.5	109.9	9.87	3.85	30	3.75	2.77	33.63	15.75	13.8	1428	610	211
sgmb1t	16.9	-26	1	6.5	87.97	11.04	5.9	30	3.88	0.51	31.82	16.08	17.2	1378	578	209
spla1l	13.6	-13	1	7	243.9	17.84	3.87	46	4.83	2.97	52.97	23.97	25	2180	941	269
spla1t	13.6	-13	1	7	218.6	12.83	5.11	46	6.43	4.09	47.32	23.85	19.3	2049	861	272

compared with records at sites close to the epicentral area exhibiting R<20Km (e.g. a399, a499, athal, mnsa, dfna, fix, sgma). This is due to the fact that, apart from the attenuation effect, distance causes a more even distribution of the energy within the duration of the event.
Another duration measure is the bracketed duration (BRD) defined as the time during which the accelerogram assumes values greater than a given level L expressed as percentage of g. In Table 1 the corresponding BRD values for L = 0, 3% and 5% of g, are given. The computed bracketed duration for two levels (3% and 5% of g) of the 42 components are plotted against the epicentral distance R (in Km) in Figs. 2a,b. Open circles correspond to sites at ground level and solid circles correspond to sites at various underground levels. Comparisons are also made with existing empirical predictions of bracketed duration of Greek accelerograms [Koutrakis, 2000]. The comparison confirms the reasonable accuracy of the empirical predictions.

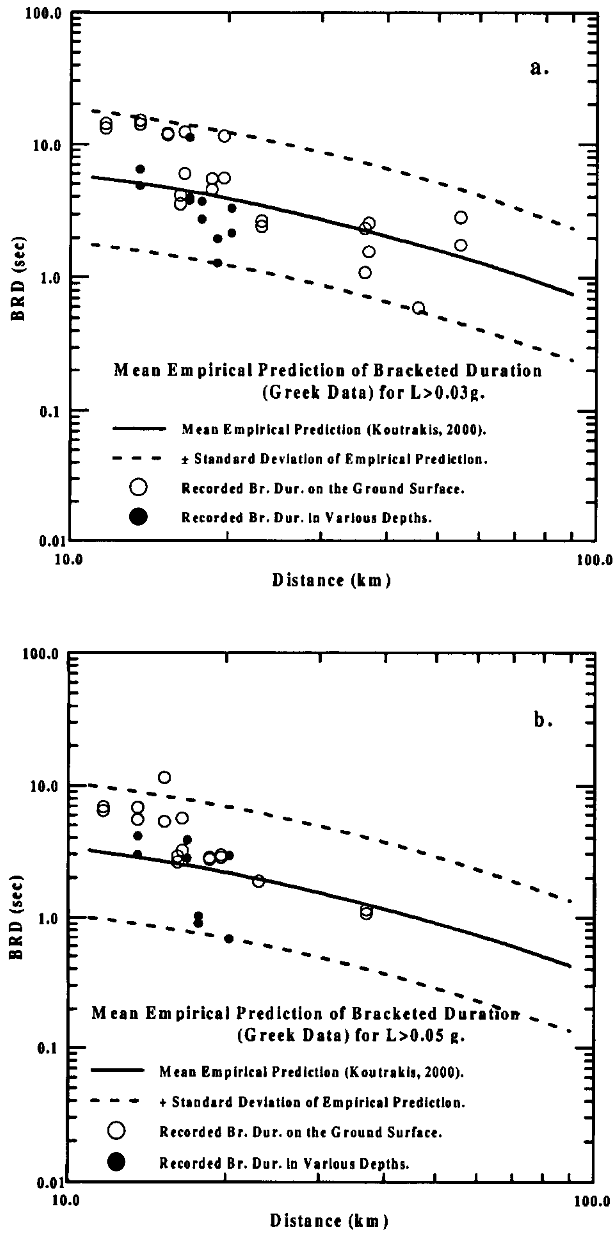

Fig. 2. The computed bracketed duration for two levels (3% and 5% of g) in comparison to mean empirical relation for Greece (Koutrakis, 2000).

ENERGY RELATED MEASURES

Among the various computed indices of the damage potential of strong ground motions, it was decided to present herein only three, as they proved [Koilopoulos *et al.*, 1998] to be more stable and reliable indicators of the damageability of Greek strong motion records. In particular, these indices are:
(a) The Housner Intensity index (I-H), taken here to be equal to the area under the 5% damped pseudo-velocity spectrum PSV for the period range 0.1s-2.5s:

$$\text{I-H} = \int_{0.1}^{2.5} PSV(T)\, dT \qquad (3)$$

In Fig. 3a the correlation between the Housner index I-H and the Modified Mercally Intensity Imm, for the 42 components is shown. Additionally, the relevant empirical regression function for Greek Data [Koliopoulos *et al.*, 1998] is presented. The agreement between predicted (solid line) and observed (circles) values is very satisfactory. No clear influence of the recording site's level (open circles corresponding to ground level sites vs solid circles corresponding to underground sites) is observed. In Fig. 3b, a similar comparison between I-H and both PGA and PGV values is shown Once again, the accuracy of the empirical regression functions is confirmed.
(b) The Total Energy Index (TEI), defined here as the average value of the total input energy of all the 5% damped oscillators with periods between 0.1s and 2.5s and expressed in terms of an equivalent velocity per unit mass

$$TEI = \sqrt{2E_t} \qquad (4)$$

Where E_t is the above mentioned, average value of the energy induced by the ground shaking into the oscillators. For each oscillator of period T_j with response x(t) under the action of ground acceleration $\alpha_g(t)$ of total duration T_W, the induced energy is equal to:

$$E(T_j) = -\int_{0}^{T_W} \alpha_g(u)\ \dot{x}(u)\, du \qquad (5)$$

In Fig. 3c computed values of TEI (open and solid circles) vs the corresponding Imm are shown. A close agreement is observed between these values and predictions (soilid line) based on the regression function proposed by Koiliopoulos *et al* [1998].
c) The earthquake ground motion potential to damage medium-period (velocity controlled) structures expressed via a measure proposed by Fajfar *et al*, [1990]. This index (I-F) results from the peak ground velocity PGV and the Husid duration as

$$\text{I-F} = PGV \cdot HuDu^{0.25} \qquad (6)$$

In Fig. 3d computed values of I-F (open and solid circles) are plotted against Imm and compared with predictions based on empirical regression function [Koliopoulos *et al.*, 1998]. Once again, a remarkable correlation between I-F and Imm is manifested and the accuracy of I-F empirical predictions is confirmed.

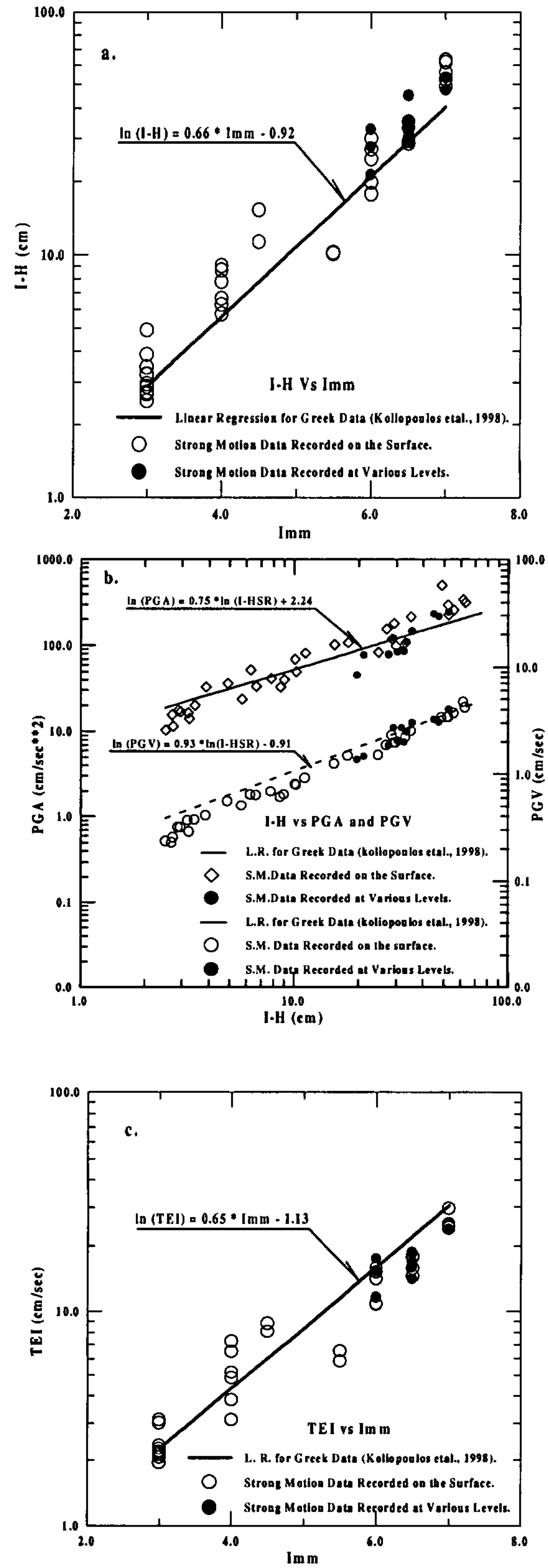

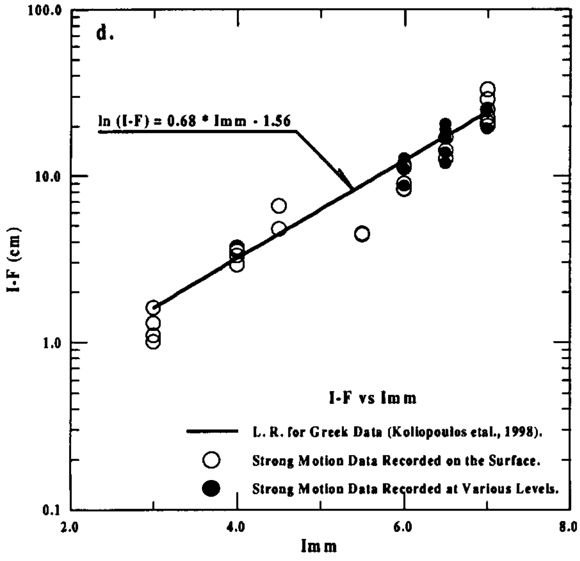

Fig. 3. Macroseismic intensity versus energy related indices: I-H (a), TEI (c) and I-F (d). Peak ground values (pga,pgv) versus I-H (b).

3D RESPONSE SPECTRA

As stated in the introduction, a promising novel concept of 3D response spectra was proposed by Safak [1998] in order to incorporate the duration into the spectral values. Following his developments, it was decided to limit the present work to the construction of 5% damped 3D pseudo velocity response spectra. For each ground motion component three groups of PSV response spectra were produced. The first group consisted of 50 PSV spectra, $PSV_j(T)$ for j=1,2,...,50 in descending order. The first $PSV_1(T)$ spectrum is identical to the conventional PSV spectrum corresponding to the absolute maximum values of the response velocity. The second $PSV_2(T)$ spectrum corresponds to the second larger peak of absolute response velocity. The third $PSV_3(T)$ corresponds to the third larger peak, and so on. A plot of the whole group of PSV spectra, forms a 3D PSV_j figure (rather than the conventional 2D PSV plot). One axis assumes values of period T, a second axis the values of index j and the third axis the PSV (T,j) value. The resulting surface PSV(T,j) starts with maximum values PSV(T,1) and decays to the minimum values PSV(T,50). The rate of the decay is indicative of the sustainability of the PSV values. Slow decay indicates a damage-prone response time history with many large amplitude peaks while a fast decay indicates less destructive time histories with few (perhaps one or two) high amplitude peaks and a large number of small amplitude peaks. This piece of information is clearly not available if only the 2D PSV spectrum is examined. The sustainability of spectral values is controlled by two characteristics. Firstly, the duration of the response time history (the longer the response record the larger the number of peaks and the probability of realization of extreme values). Secondly, the frequency contents of the response process (the smaller the bandwidth of the process the higher the probability of realization of high amplitude peaks). Safak [1998] has reported that if two records with similar properties (e.g. similar conventional 2D response spectra) but of different duration are examined and the two 3D PSV_j spectra for j=1,20 compared, the difference in duration will be visually manifested. Furthermore, the volume under the 20 component PSV(T, j=1,20) surface, produces a 3D spectral intensity measure which appeared to correlate well with damage indices computed via the nonlinear damage analysis program IDARC for a ten-story model building subjected to a total of 375 records from Northridge earthquake. No justification was provided however, as to the choice of the number of spectral components (i.e. j = 20). Additionally, the observed differences in the 3D response spectra due to duration variability, resulted from artificially generated records and the applicability of the visual inspection to real strong motion records required some further validation.

To address the above issues, the sensitivity of the computed 3D PSV spectra on the choice of j, was firstly examined. 3D plots for j=20 and j=50 were compared. The comparison revealed that, for the sample of records considered herein, no additional information is produced by increasing the components from 20 to 50. To further explore this issue, the volumes under the 20 component (solid stars) and 50 component (open circles) 3D PSV spectra were computed and plotted against Imm (Fig. 4a), I-H (Fig. 4b), TEI (Fig. 4c) and I-F (Fig. 4d).

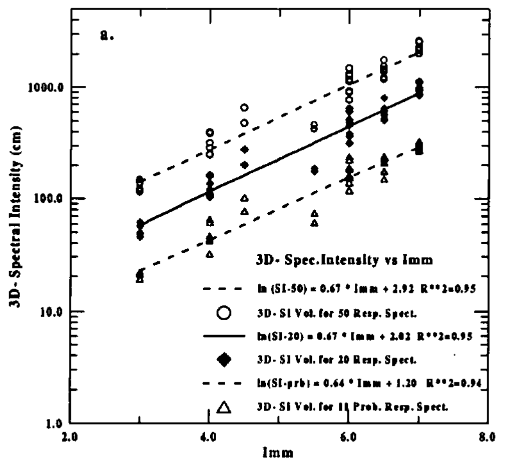

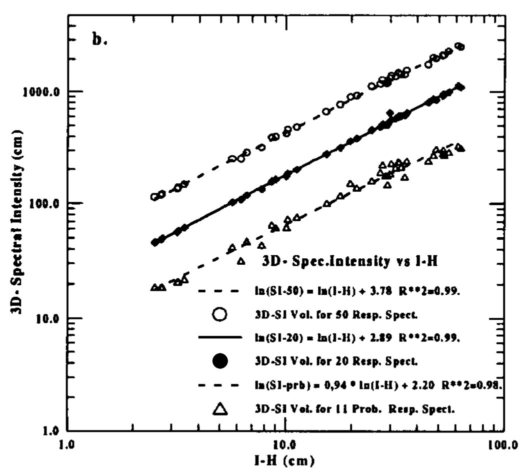

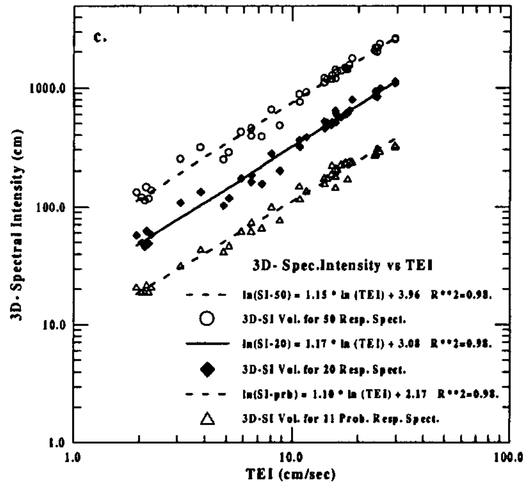

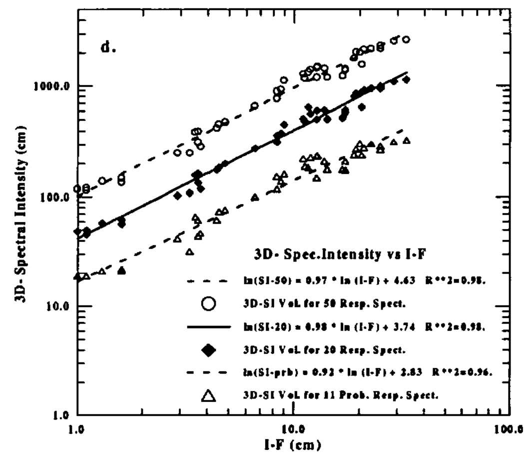

Fig.4. 3D spectral Intensity versus macroseismic Intensity (a), and energy related indices : I-H (b), TEI (c) and I-F (d)

All figures, confirm that the 3D spectral intensity measure (i.e. the volume under the 3D PSV spectra) correlates well with the energy related available measures, but this correlation is insensitive to the choice of j.

This finding is not surprising, as a visual inspection of the 3D PSV spectra corresponding to actual (not simulated) records manifest a remarkable sustainability. The increase of volume therefore, is almost proportional to the increase of the number of components j. Hence, under these conditions, no useful information is added by increasing j. This remark also explains the excellent correlation between the 3D spectral intensity and the Housner index, I-H, because the former tends to become a multiple of the latter. Given the fact that I-H exhibits strong correlation with Imm and the rest of energy indices (TEI, I-F), is not surprising that the same pattern is also true for the 3D spectral intensity.

In order to overcome the arbitrariness of the choice of j, a second group of probabilistic 3D PSV spectra was produced. Each 3D spectrum consists of 11 2D components with constant probability of exceedence. The first component is identical to the conventional 2D PSV including the values of the response process with probability of exceedence 0%. The second component is the 2D PSV spectrum produced by the amplitudes of the response process with a probability of exceedence 1%. The third component corresponds to amplitudes with probability of exceedence 2%, and so on. Using the notation PSV(T,Pr.[j%]) this second group comprises the components PSV(T,Pr.[j%]) for j=0,..,10. A third group was also constructed from the mean values of the upper 1%, 2%, ..., 10% of the response amplitude levels, but due to space restrictions the findings concerning this third group will not be addressed herein.

The adoption of probability based 3D spectra sets in a somewhat more rigorous basis the choice of the 2D components. Furthermore, it offers an opportunity to distinguish between records with the same number of peaks (perhaps due to similar duration) but different frequency content which greatly influences the tails of the distribution. Examples of probabilistic 3D PSV spectra are shown in Figs. 5a, 5b and 5c. It is apparent that the visual inspection of sustainability is facilitated. It is additionally observed that the probabilistic 3D spectral intensities (computed as the volume under the probabilistic 3D PSV spectra and shown as open triangles) exhibit comparable correlation with their deterministic counterparts, when plotted against Imm (Fig.4a), I-H (Fig.4b), TEI (Fig.4c) and I-F (Fig. 4d). As it will be shown later, another advantage of the use of the probabilistic 3D-PSV is that the influence of local soil conditions (frequency content) in the damage potential of the excitation can be deduced.

Consider, for example, the components a499-11 and kert99-11. Comparing the values of PGA, PGV and duration, one could draw the conclusion that the former ground motion is considerably less destructive than the latter. From an engineering point of view, the same conclusion is drawn from a comparison of the conventional PSA response spectrum (Fig. 6). For a nonlinear time-domain dynamic structural analysis therefore, the designer would probably be advised to select the kert99-11 record. An examination of the energy related indices (I-H, TEI, I-F) however, reveal that the damage potential of the two records is comparable. This is further confirmed by the comparison of both deterministic and probabilistic 3D spectral intensity measures of the two records. This, perhaps surprising, result can be fully explained by a simple visual inspection of the corresponding probabilistic 3D-PSV spectra in Figs. 5a and 5b. The sustainability of the a499-11 spectral values is far greater than the sustainability of the corresponding spectral values of the kert99-11 record. Given that the duration of the latter is greater than the duration of the former component, the sustainability can be solely attributed to the frequency content of the two records. Indeed KERT-site is classified as rock while the A4-site as firm soil conditions.

Another example of the use of 3D response spectra in order to demonstrate and quantify the destructiveness of strong ground motion, is taken by considering the records kert99-11 and mnsa11.

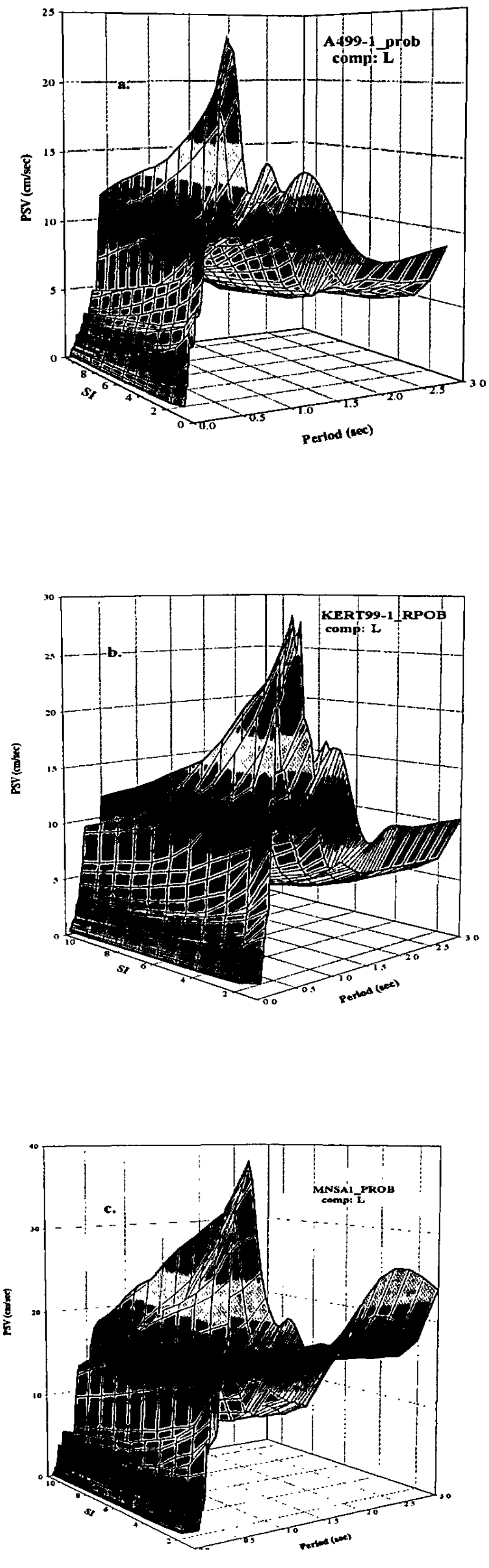

Fig. 5. Probabilistic 3D PSV spectra corresponding to 3 different accelerographic sites.

Here we have two ground motion records with comparable peak ground motion values (PGA, PGV) but with energy related and 3D spectral intensity indices which suggest a far greater damage potential of the latter record. A comparison of the 3D-PSV plots in Figs. 5b and 5c, reveals a fast decay of the spectral values corresponding to the kert99-11 record (rock site) and a slow decay of the spectral values corresponding to the mnsa11 record (soft soil site).

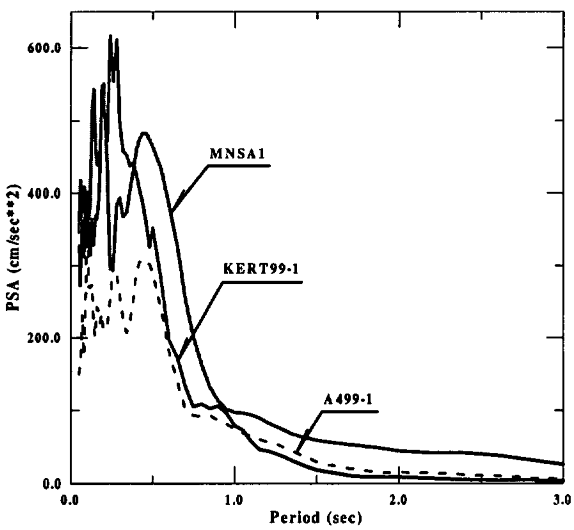

Fig. 6. Acceleration response spectra corresponding to the three accelerographic sites as in Fig.5

CONCLUSIONS

The duration and energy characteristics of 42 horizontal strong ground motion components appear to correlate well with recently developed empirical predictions of these parameters for Greek data [Koiliopoulos *et al*, 1998; Koutrakis, 2000]
A novel [Safak, 1998] 3D response spectrum technique has been implemented and restated in a more rigorous basis within a probabilistic framework. The suggested new probabilistic version of the 3D spectral concept provides the means for a more rational classification of ground motion records in terms of damage potential. The role of duration and local soil conditions in the sustainability of the spectral values and the destructiveness of the strong ground motion can be easily identified through either the energy related indices or the 3D response spectra. It is hoped that this additional information (currently not available in the conventional response and design spectra) will be incorporated – to a certain extent – in future code provisions.

ACKNOWLEDGEMENTS

The authors wish to acknowledge the financial support by the Technological Education Institute of Serres (Research fund No. 8/18-11-1998).

REFERENCES

Anastasiadis, A., M. Demosthenous, C. Karakostas, N. Klimis, B. Lekidis, B. Margaris, C. Papaioannou, C. Papazachos and N. Theodulidis. [1999]. AThe Athens (Greece) Earthquake of September 7, 1999: Preliminary Report on Strong Motion Data and Structural Response.@ MCEER Bulletin, 3, pp. 1-6.
Chapman, M.C. [1999]. AOn the use of elastic energy for seismic hazard analysis@, Earthquake Spectra, 15, pp. 607-635.
Fajfar, P., T. Vidic and M. Fischinger. [1990]. AA measure of earthquake motion capacity to damage medium-period structures.@, Soil Dyn. Earthq. Engrg., 9, pp. 236-242.
Koliopoulos, P.K., B.N. Margaris and N. S. Klimis. [1998]. ADuration and energy characteristics of Greek strong motion records.@, J. Earthq. Engrg., 2, pp. 391-417.
Koutrakis, S. [2000]. AStudy of the duration of strong motion in Greece@ MSc Thesis,Aristl. Univ.of Thessaloniki, pp 1-99.
Psycharis, I., D. Papastamatiou, I. Taflambas and P. Carydis. [1999]. ALearning from earthquakes : The Athens, Greece Earthquake of September 7, 1999.@, EERI Special Earthquake Report, pp. 1-8.
Safak, E. [1998]. 3D Response Spectra : AA method to include duration in response spectra, CDRom-Proc@ Eleventh Europ. Conf. on Earthq. Engrg. Paris 1998,pp 1-9
Uang, C.-M. and V.V. Bertero [1990]. AEvaluation of seismic energy in structures.@, Earthq. Engrg. Struct. Dyn., 19, pp. 77-90.